

## Recent Progress in Developing New Rare Earth Materials for Hole Burning and Coherent Transient Applications

Y. Sun<sup>a</sup>, C. W. Thiel<sup>a</sup>, R. L. Cone<sup>a</sup>, R. W. Equall<sup>b</sup>, R. L. Hutcheson<sup>b</sup>

<sup>a</sup>*Department of Physics, Montana State University, Bozeman, MT 59717, USA*

<sup>b</sup>*Scientific Materials Corporation, 310 Icepond Road, Bozeman, MT 59715, USA*

### Abstract

To develop new spectral hole burning materials and optimize known materials for applications such as optical correlator and memory devices, a broad range of experiments, from optical coherent transients to photoelectron spectroscopy, have been used to elucidate fundamental aspects of the rare-earth electronic structure. We report progress in the characterization of  $\text{Er}^{3+}$  doped materials where we have measured an ultra-narrow linewidth of 50 Hz in  $\text{Er}^{3+}:\text{Y}_2\text{SiO}_5$  and a  $\Gamma_{\text{inh}}/\Gamma_{\text{h}}$  ratio as high as  $10^8$  in  $\text{Er}^{3+}:\text{LiNbO}_3$ . Progress is also reported for  $\text{Nd}^{3+}:\text{YVO}_4$  where the high oscillator strength is an advantage over other rare earth ions and excellent coherence properties can be achieved at modest magnetic fields. Finally we report advances in the pursuit of photon-gated hole burning materials through the study of the energies of the localized rare earth energy states relative to the host band states, providing the foundation for understanding photoionization in these materials.

**Keywords:** rare earths, coherent transients,  $\text{Nd}^{3+}:\text{YVO}_4$ , photon-gated hole burning, photoemission,  $\text{Er}^{3+}$

**PACS:** 71.55.-i, 42.70.-a, 42.70.Ln

Corresponding Author: Y. Sun  
Address: Physics Department EPS 264, Montana State University,  
Bozeman, Montana 59717, USA  
Phone: 1 406 994 6163  
Fax: 1 406 994 4452  
E-mail: sun@physics.montana.edu

## 1. Introduction

Rare earth spectroscopy has been one of the cornerstones in the development of hole-burning techniques, and rare earth materials have found numerous applications in hole burning and coherent transient applications. In this short paper we present a few of the recent developments in our search for new rare earth materials with optimum optical properties.

Of the numerous applications proposed for hole burning materials, optical correlators and memory devices have had a prominent position. The  $1.5 \mu\text{m}$   $^4\text{I}_{15/2} \leftrightarrow ^4\text{I}_{13/2}$  transitions of  $\text{Er}^{3+}$  materials provide exciting possibilities for accelerating the development of practical hole burning technologies by incorporating the established telecommunications equipment infrastructure that operates in this same spectral band. These wavelengths are also ‘eye safe,’ opening additional applications. Toward this goal, in Sec. 2 we report the progress made in the study of  $\text{Er}^{3+}$  doped  $\text{Y}_2\text{SiO}_5$  (YSO),  $\text{Y}_2\text{O}_3$ ,  $\text{YAlO}_3$ , YAG,  $\text{CaWO}_4$ , and  $\text{SrWO}_4$  samples.

Another important factor in these applications is the oscillator strength of the optical transition. For the forbidden rare earth  $4f^N$  to  $4f^N$  transitions, the oscillator strengths are generally small ( $\sim 10^{-6}$ - $10^{-9}$ ); however, the  $\text{Nd}^{3+}$   $^4\text{I}_{9/2} \rightarrow ^4\text{F}_{3/2}$  transition has one of the largest oscillator strengths among all the rare earth transitions of practical interest for applications. The coherence properties of this transition in the particular case of  $\text{Nd}^{3+}:\text{YVO}_4$  are discussed in Sec. 3.

For many applications, the robustness of the spectral hole can be critical to enable practical devices to be developed. Photon-gated hole burning has been proposed as a solution to this problem; however, materials appropriate for technological applications are currently not available. For photon-gated photoionization hole burning in rare earth doped inorganic insulators, an understanding of the energy level structure of the  $4f^N$  levels relative to the host band states is required to successfully develop efficient materials and to determine the optimum photon energies for the gating process. Recently, using photoemission spectroscopy and synchrotron radiation, we have measured the  $4f^N$  ground state energies relative to the host valence band for several rare earth doped garnets, including YAG.[1,2] This work has led to the development of empirical models for describing the relative energies of the  $4f^N$  and  $4f^{N-1}5d^1$  states of the rare earth ions in rare earth activated materials. In section 4, we report the application of this information to the development of photon-gated hole burning materials, with new results for rare earth doped  $\text{YAlO}_3$  given as a concrete example.

## 2. $\text{Er}^{3+}$ Materials

Photon echoes, stimulated photon echoes, and other characterization measurements have been carried out on the  $^4\text{I}_{15/2} \leftrightarrow ^4\text{I}_{13/2}$  transition  $\text{Er}^{3+}$  in a range of oxide crystals. This transition occurs in the  $1.5 \mu\text{m}$  region, coinciding with the telecommunications band. The properties of this transition were examined for materials including  $\text{Y}_2\text{SiO}_5$ ,  $\text{Y}_2\text{O}_3$ ,  $\text{LiNbO}_3$ , YAG,  $\text{YAlO}_3$ ,  $\text{CaWO}_4$ , and  $\text{SrWO}_4$ .

In these materials,  $\text{Er}^{3+}$  was doped at very low concentration ( $\sim 10$  ppm) to minimize dephasing and spectral diffusion induced by Er-Er interactions. The coherence properties for 0.005%  $\text{Er}^{3+}:\text{YSO}$  have been reported earlier where the dephasing time  $T_2$  was measured to be as long as  $580 \mu\text{s}$ . [3]

To further reduce the Er-Er dephasing, we examined an even more dilute 0.001% Er<sup>3+</sup> doped sample. For this sample, the dephasing time was measured to be as long as 6.4 ms at B=70 kG and T=1.5 K, corresponding to a homogeneous linewidth  $\Gamma_h$  of ~50 Hz. The large g-factor of Er<sup>3+</sup> in this material allows the Er-Er spin-flip induced dephasing to be frozen out at moderate magnetic field. At a typical field achieved using simple button-sized Nd-Fe-B magnets (2.5 kG), the Er-Er induced dephasing is suppressed enough that the homogeneous linewidth is as narrow as  $\Gamma_h \sim 2.5$  kHz.

The Y<sub>2</sub>O<sub>3</sub> host is another low nuclear magnetic moment material similar to YSO. However, because of the higher symmetry of the crystal ( $T_h$ ), in addition to the two crystallographically inequivalent Er<sup>3+</sup> sites, there are also six magnetically inequivalent site orientations for the C<sub>2</sub> site and four magnetically inequivalent site orientations for the C<sub>3i</sub> site. Measurements of the coherence properties of the C<sub>2</sub> site showed that they are similar to the properties observed in YSO, with a comparable narrowing of the homogeneous line observed for applied magnetic fields. For the 0.005% Er<sup>3+</sup>:Y<sub>2</sub>O<sub>3</sub> sample, very strong photon echoes were observed even in a magnetic field as weak as a few hundred Gauss.

In the search for materials with large inhomogeneous to homogeneous linewidth ratios  $\Gamma_{inh}/\Gamma_h$ , 0.06% Er<sup>3+</sup>:LiNbO<sub>3</sub> has proven to be of particular interest. We have found that this material has a large inhomogeneous linewidth of  $\Gamma_{inh} = 250$  GHz, and a homogeneous linewidth as narrow as  $\Gamma_h = 4$  kHz at 1.5 K for B=5 kG along the crystal's c-axis. Increasing the magnetic field strength results in a further narrowing of the homogeneous linewidth, reaching a limit of 2 kHz for a field of 20 kG along the c-axis. These properties correspond to  $\Gamma_{inh}/\Gamma_h$  greater than 10<sup>8</sup>, making this an interesting material for spatial-spectral holographic applications where a large  $\Gamma_{inh}/\Gamma_h$  determines the time-bandwidth product for signal processing. The homogeneous linewidth was also measured across the inhomogeneous absorption profile by shifting the laser to excite at every 10 GHz interval, revealing that the homogeneous linewidth  $\Gamma_h$  is constant across the entire inhomogeneous line.

In Table I we present all the coherence parameters discussed above, as well as the transition wavelengths and the  $\Gamma_{inh}/\Gamma_h$  ratio as a measure of the time-bandwidth product. We have found that for those applications where low field is a prerequisite, the YSO and Y<sub>2</sub>O<sub>3</sub> hosts provide excellent candidates, while applications that require very high bandwidth would benefit from the properties of materials such as LiNbO<sub>3</sub>. In addition, the properties of Er<sup>3+</sup> doped YAlO<sub>3</sub>, YAG, CaWO<sub>4</sub>, and SrWO<sub>4</sub> were studied and given in Table I. Lengthening of T<sub>2</sub> with the magnetic field was also observed in these materials. All materials have similar oscillator strength except for Er:SrWO<sub>4</sub> where it was an order of magnitude smaller than the other materials.

### 3. Nd<sup>3+</sup> materials

In the search for new materials with higher oscillator strength, we have studied the Nd<sup>3+</sup>:YVO<sub>4</sub> <sup>4</sup>I<sub>9/2</sub> - <sup>4</sup>F<sub>3/2</sub> transition at 879.705 nm (11364.4 cm<sup>-1</sup>). The upper <sup>4</sup>F<sub>3/2</sub>(R<sub>1</sub>) level is the lasing level for the renowned 1.06  $\mu$ m Nd<sup>3+</sup> lasers. The <sup>4</sup>I<sub>9/2</sub>(1) - <sup>4</sup>F<sub>3/2</sub>(1) transition was very strongly  $\pi$  polarized and over absorbing at the center of the absorption line. The weakly absorbing  $\sigma$  polarization has a linewidth of 0.9 GHz. For this sample, the total absorption strength is 3.4 cm<sup>-1</sup>/cm, corresponding

to a calculated oscillator strength of  $f = 8 \times 10^{-6}$ . This value can be compared with the well known oscillator strength of the  ${}^4\text{H}_6(1) \rightarrow {}^4\text{H}_4(1)$  transition of  $\text{Tm}^{3+}:\text{YAG}$ , where a 0.1% doped sample exhibits a total absorption of  $1.6 \text{ cm}^{-1}/\text{cm}$ . [4] Thus, we see that for similar concentrations, the absorption strength of  $\text{Nd}^{3+}:\text{YVO}_4$  is more than 200 times larger than the commonly used  $\text{Tm}^{3+}:\text{YAG}$  transition. This increase in absorption strength results from a combination of the higher oscillator strength of the  $\text{Nd}^{3+}$  transition and the highly polarized nature of the transition in the uniaxial host  $\text{YVO}_4$ .

In this material, the electronic magnetic moment of the ground state can be characterized by  $g$ -factors of  $g_{\parallel} = 0.91$  and  $g_{\perp} = 2.36$ , and the excited state has  $g_{\perp} \approx 0.5$ . In a magnetic field along the crystal's  $a$ -axis, the transition probabilities between all Kramers components are essentially identical; thus, the oscillator strength between the levels split by a magnetic field is estimated to be  $4 \times 10^{-6}$ .

Photon echo experiments were carried out in an Oxford Spectromag Cryostat with a sample of 0.001%  $\text{Nd}^{3+}:\text{YVO}_4$  that was 0.68 mm thick along the  $a$ -axis. Two pulse echoes were excited using a Ti:sapphire laser gated by two acousto-optical modulators (A/O). Pulses were 100 ns long due to the limits imposed by the rise and fall times of the A/O's used in the experiment. Particular care was taken to ensure that the pulse areas were less than  $\pi/2$ . The photon echoes were detected using a silicon PIN diode with no optical gating in front of it.

No echo was observable in fields below 1 kG. Beginning at 1.5 kG, an echo can be observed with an echo decay curve that modulates strongly due to the quantum interference between transitions involving different components of the superhyperfine structure. This modulation is reduced at higher magnetic fields as the hyperfine splittings become larger than the Fourier linewidth of the pulses. This modulation effect makes it difficult to determine the exact dephasing time at lower fields. Typical decay curves are shown in Figure 1.

The dephasing time  $T_2$  lengthens (with a corresponding narrowing of  $\Gamma_h$ ) as the applied field is increased as shown in Figure 2. This lengthening of  $T_2$  is similar to what is expected from Nd-Nd spin flip induced dephasing as estimated from the ground state  $g$ -factor of 2.36. In a field larger than 15 kG, the dephasing is in the "superhyperfine limit" where the dephasing is defined by the interaction between the  $\text{Nd}^{3+}$  and the surrounding vanadium nuclei.

Three pulse echo experiments were also carried out in this system. We found that relatively weak spectral diffusion was observed over a 5 ms time scale, and stimulated echo decays have been found to have two different decay constants, a  $37.5 \mu\text{s}$  component due to the upper state lifetime and a 3.3 ms component corresponding to the ground state Zeeman sublevel storage time. The initial intensity of the slower second component was about ~3% of the fast component.

#### 4. The search for photon-gated hole burning materials

Many proposed technological applications of persistent spectral hole burning are enabled by the large  $\Gamma_{\text{inh}}/\Gamma_h$  ratios that may be achieved for the  $4f^N$  to  $4f^N$  transitions of the trivalent rare earth ions doped into inorganic insulators. In addition to the need for excellent coherence properties, many

applications would greatly benefit from a mechanism for probing the population distribution of the optical transition without perturbing the population through further hole burning. Photon-gated hole burning provides a mechanism for non-destructive readout by employing a process that requires two photons of different frequencies. One such process is two-step photoionization hole burning: the first photon generates a population distribution in the  $4f^N$  to  $4f^N$  optical transition and the second photon photoionizes the population in the excited state, permanently removing them from the absorption.[5,6] Thus, when the second photon is present, information may be "written" into the rare earth ions' population; when the second photon is not present, the information may be read back without the partial erasure associated with non-gated hole burning mechanisms.

Direct photoionization of highly localized  $4f^N$  states is generally a very weak process for trivalent rare earth ions. The limited spatial overlap between the host conduction band states and the localized rare earth states implies the need for a more spatially extended intermediate state, such as  $4f^{N-1}5d^1$ , for efficient ionization. Efficient excitation of rare earth ions into the  $4f^{N-1}5d^1$  state is made possible by the large cross-section of the parity allowed transition from the upper  $4f^N$  state involved in the hole burning to the  $4f^{N-1}5d^1$  state and the long  $4f^N$  lifetimes. However, for ionization to occur, the excited  $4f^{N-1}5d^1$  state must have an absolute energy above the host conduction band so that the 5d electron may relax into a conduction band state. If deep electron trap states are present in the lattice, the mobile electrons in the conduction band may become trapped away from the ionized rare earth ion, providing a mechanism for permanent hole burning.

To determine the second-step photon energy needed to photoionize the rare earth ion, the energy of the rare earth ion's states relative to the host band states must be measured. Recently, we have employed the techniques of resonant and conventional electron photoemission spectroscopy to determine the energy of the  $4f^N$  ground states relative to the host crystal's valence band.[1,2] Combined with the host band gap and  $4f^{N-1}5d^1$  transition energies obtained from ultraviolet spectroscopy, these measurements can be used to locate the energies of the  $4f^{N-1}5d^1$  states relative to the host conduction band.

It is well known that  $YAlO_3$  forms both stable and transient color centers under ultraviolet irradiation,[7] indicating the presence of deep trap states in the lattice. The abundance of electron trap states and the excellent optical properties of rare earth doped  $YAlO_3$  suggest that it would be a good candidate for photoionization hole burning. With this motivation, the rare earth energy levels were located relative to the host band states for rare earth doped  $YAlO_3$ , as shown in Fig. 3. Resonant photoemission spectroscopy was used to measure the  $4f^N$  energy of  $Tb^{3+}$  relative to the valence band and to determine the absolute energy of the valence band maximum in  $YAlO_3$ . This work was carried out on the Iowa State/Montana State ERG/Seya beam line at the University of Wisconsin-Madison Synchrotron Radiation Center using the apparatus and techniques described in Ref. [1]. The  $4f^N$  energies of  $Ce^{3+}$  and  $Lu^{3+}$  were determined by applying the techniques developed in ref [1] to analyze the x-ray photoemission spectra published in ref [8]. Using the empirical model for the  $4f^N$  binding energies described in Ref. [1], these measured energies (circles in Fig. 3) allow the  $4f^N$  energies of the remaining rare earth ions to be accurately predicted, as shown by the solid line in Fig. 3. These results predict that, among the trivalent rare earth ions, only  $Ce^{3+}$  and  $Tb^{3+}$  have  $4f^N$  ground state energies above the host valence band. This has important implications for choosing an active ion for photon-gated hole burning. Ions with their  $4f^N$  ground state energy

degenerate with valence band states are unlikely to form stable tetravalent ions after photoionization since higher energy valence band electrons would rapidly relax into the lower energy  $4f^N$  state, returning the ion to a trivalent state and making them poor candidates for efficient photoionization hole burning materials. Thus, since the  $4f^N$  to  $4f^N$  transitions of  $Ce^{3+}$  are not easily accessible,  $Tb^{3+}$  represents the best candidate for photon-gated hole burning in  $YAlO_3$ .

The energies of the  $4f^7 5d^1$  states were determined from the ultraviolet absorption of  $Tb^{3+}:YAlO_3$  for energies up to  $57000\text{ cm}^{-1}$ . Four  $4f^8$  to  $4f^7 5d^1$  transitions were observed within this range: the lowest energy transition observed was a weak spin-forbidden transition at  $42930\text{ cm}^{-1}$  (a high-spin  $4f^7 5d^1$  state), while intense spin-allowed transitions were observed at  $46060\text{ cm}^{-1}$ ,  $48060\text{ cm}^{-1}$ , and  $50500\text{ cm}^{-1}$  (low-spin  $4f^7 5d^1$  states). These energies are indicated in Fig. 3 by the triangles. The lowest energy  $5d^1$  state of  $Ce^{3+}$ , determined using results from ref [9], is also indicated in Fig. 3. In addition, estimates for the lowest  $4f^{N-1} 5d^1$  states of the remaining ions are indicated by the dotted lines in Fig. 3, where the lower and upper dotted lines for the second half series indicate the energies of the high-spin and low-spin  $4f^{N-1} 5d^1$  states, respectively. These estimates were obtained by combining the model[1] for the  $4f^N$  ground state binding energies with the model and parameters of Dorenbos [10,11] for estimating the lowest  $4f^{N-1} 5d^1$  transitions in a material. The  $4f^{N-1} 5d^1$  binding energies represent the relative energies required to remove the  $5d$  electron from the  $4f^{N-1} 5d^1$  states of the trivalent rare earth ions in  $YAlO_3$ . These energies show only a weak variation of less than 1 eV across the rare earth series, indicating that the absolute energies of the  $5d$  electrons are nearly constant for the lowest  $4f^{N-1} 5d^1$  states of the trivalent ions in  $YAlO_3$ .

To locate these states relative to the host conduction band, the host band gap energy is required. The fundamental band gap of  $YAlO_3$  is estimated to be 8.0 eV from optical absorption and reflectivity measurements.[12] This gives an estimate of 7.5 eV for the direct photoionization threshold of  $Tb^{3+}$ , with all of the observed  $4f^7 5d^1$  states lying significantly below the bottom of the host conduction band. Thus, if the blue  ${}^7F_6$  to  ${}^5D_4$  transition at  $20562\text{ cm}^{-1}$  in  $YAlO_3$  was used as the hole burning transition, a second 4.9 eV gating photon would be required to directly photoionize the excited  $Tb^{3+}$  ion. Since no  $4f^7 5d^1$  level was observed at this energy, an even greater energy would be required to excite to an upper lying  $4f^7 5d^1$  state within the conduction band. These results suggest that  $YAlO_3$  would present an inconvenient choice for a photon-gated hole burning material.

By applying these methods to additional materials, potential candidates for photoionization hole burning in inorganic materials may be identified and analyzed. Precise knowledge of the energy level structure, including the host band states, provides insight into these materials and the photoionization process, allowing a material's performance, or lack of performance, to be quantitatively characterized. This insight can be used to understand current photon-gated hole burning materials as well as to motivate the logical development of new materials. This information is also important for the design of efficient phosphors and scintillators.

## Acknowledgments

We thank Marco Bettinelli of the Università degli Studi di Verona, Italy, who supplied the 0.001%  $Nd^{3+}:YVO_4$  sample, and Sebastien Ermeneux for optical spectroscopy and optically detected magnetic resonance studies of this material. The authors wish to thank G. J. Lapeyre for

contributing expertise and equipment for the photoemission experiments and R. M. Macfarlane for valuable discussions of  $\text{YAlO}_3$ . Funding for this research was provided in part by the Air Force Office of Scientific Research under Grant Nos. F49620-97-1-0411, F49620-98-1-0171, and F49620-00-1-0314. This work was also partially supported under a National Science Foundation Graduate Research Fellowship. Part of the work presented here was conducted at the Synchrotron Radiation Center, University of Wisconsin-Madison, which is supported by the NSF under Award No. DMR-0084402.

## References

- [1] C. W. Thiel, H. Cruguel, Y. Sun, G. J. Lapeyre, and R. L. Cone, H. Wu, R. W. Equall, and R. M. Macfarlane, *Phys. Rev. B.* 64 (2001) 085107.
- [2] C. W. Thiel, H. Cruguel, Y. Sun, G. J. Lapeyre, R. M. Macfarlane, R. W. Equall, and R. L. Cone, *J. Luminescence* 94-95, (2001) 1.
- [3] R. M. Macfarlane, T. L. Harris, Y. Sun, R. L. Cone, and R. W. Equall, *Opt. Lett.* **22** (1997) 871.
- [4] Y. Sun, G. M. Wang, R. L. Cone, R. W. Equall, and M. J. M. Leask, *Phys. Rev. B* 62 (2000) 15443.
- [5] G. Wittmann and R. M. Macfarlane, *Opt. Lett.* 21 (1996) 426.
- [6] R.M. Macfarlane and G. Wittmann, *Opt. Lett.* 21 (1996) 1289.
- [7] A. Matkovski, A. Durygin, A. Suchocki, D. Sugak, G. Neuroth, F. Wallrafen, V. Grabovski, and I. Solski, *Opt. Mater.* 12 (1999) 75.
- [8] C. Dujardin, C. Pedrini, J. C. Gâcon, A. G. Petrosyan, A. N. Belsky, and A. N. Vasil'ev, *J. Phys.: Condens. Matter* 9 (1997) 5229.
- [9] M. J. Weber, *J. Appl. Phys.* 44 (1973) 3205.
- [10] P. Dorenbos, *J. Lumin.* 91 (2000) 91.
- [11] P. Dorenbos, *J. Lumin.* 91 (2000) 155.
- [12] T. Tomiki, F. Fukudome, M. Kaminao, M. Fujisawa, and Y. Tanhara, *J. Phys. Soc. Japan* 55 (1986) 2090.

Table I. Summary of the  $\text{Er}^{3+}$  doped oxide materials parameters. The dephasing times were presented as parameters to the Mims' decay,  $I = I_0 \exp(-4t/T_M)^x$ .  $T_M$  has its equivalence with  $T_2$ .

Material, Er conc.	Wavelength (nm)	$\Gamma_{\text{inh}}$ (GHz)	$H_0=0$		Saturated value in magnetic field		
			$T_M$ ( $\mu\text{s}$ )	$x$	$T_M$ ( $\mu\text{s}$ )	$x$	$\Gamma_{\text{inh}} / \Gamma_{\text{h}}$
$\text{Y}_2\text{SiO}_5$ , 0.001%	1536.14, site 1 1538.57, site 2	0.5	3.3	1	>2000	1.0	$3 \times 10^6$
$\text{Y}_2\text{O}_3$ , 0.005%	1535.28 nm	1	18	1.85	105	1.4	$3 \times 10^5$
$\text{LiNbO}_3$ , 0.06%	1531.52 nm	200			170	2.0	$1 \times 10^8$
$\text{YAlO}_3$ , 0.005%	1514.38 nm	1			265	2.2	$8 \times 10^5$
$\text{CaWO}_4$ , 0.005%	1532.30 nm	1			140	1.5	$4.4 \times 10^5$
$\text{SrWO}_4$ , 0.05%	1533.55 nm	1			72	1.0	$2.2 \times 10^5$
YAG, 0.1%	1526.97 nm	30			75	1.5	$7 \times 10^6$

## Figures

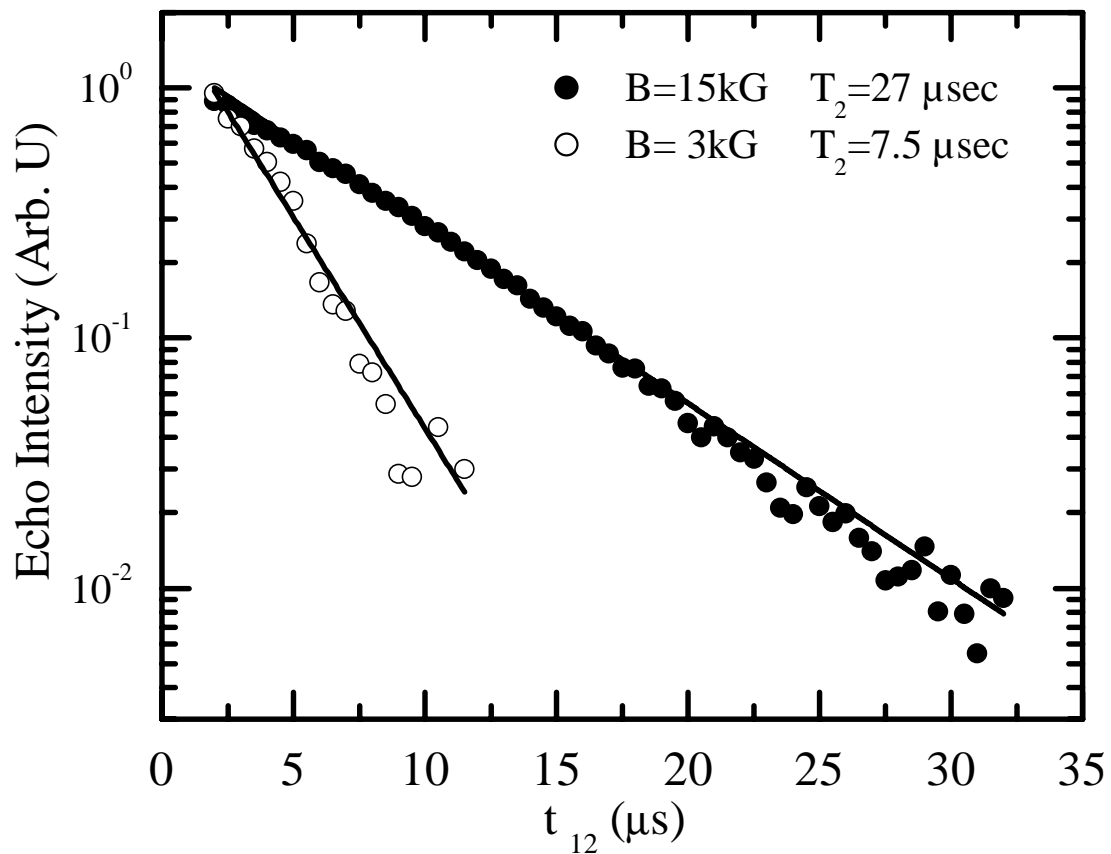


Fig. 1. Two pulse photon echo decay curves for 0.001%Nd<sup>3+</sup>:YVO<sub>4</sub> at two different values of the applied magnetic field. The magnetic field was along the a-axis. The excitation pulse widths were 100 ns.

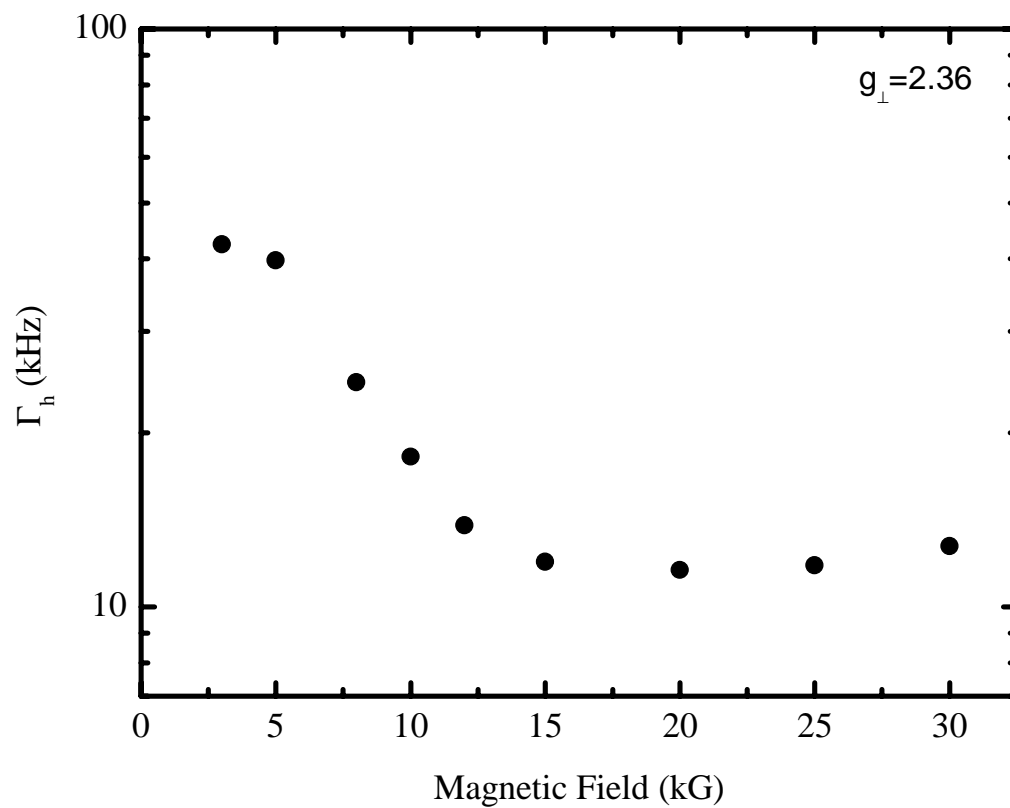


Fig. 2. Homogeneous line width at 1.5 K as a function of magnetic field applied along the a-axis for the 0.001%Nd<sup>3+</sup>:YVO<sub>4</sub> sample.

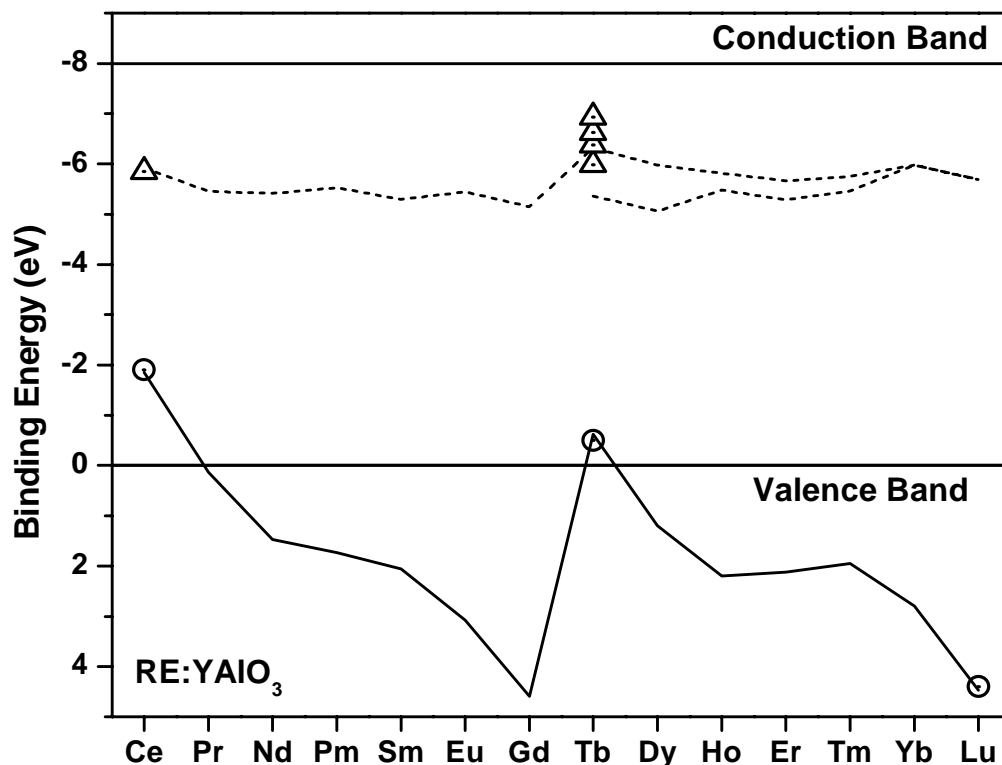


Fig. 3. Systematic behavior of 4f and 5d electron binding energies relative to host bands for trivalent rare-earth ions in YAlO<sub>3</sub>. Circles represent measured 4f binding energies of the 4f<sup>N</sup> ground states and triangles represent measured 5d binding energies for the lowest energy 4f<sup>N-1</sup>5d<sup>1</sup> states. The solid line is the model for the 4f binding energies and the dotted line is the model for the 5d binding energies. For the second half-series, the lower and upper dotted lines represent the barycenters of the lowest energy high-spin and low-spin 4f<sup>N-1</sup>5d<sup>1</sup> levels, respectively.